

SrTiO₃ substrates capped with a GaAs monolayer: An *ab initio* studyFrançois Bottin^{1,2,*} and Fabio Finocchi^{1,†}¹*Institut des NanoSciences de Paris, UMR CNRS 7588, Universités Pierre et Marie Curie and Denis Diderot, Campus de Boucicaut, 140 rue de Lourmel, 75015 Paris, France*²*Département de Physique Théorique et Appliquée, CEA/DAM Ile-de-France, Boîte Postale 12, 91680 Bruyères-le-Châtel Cedex, France*

(Received 1 June 2007; published 24 October 2007)

The epitaxy of GaAs monolayers on SrTiO₃ substrates is studied by extensive first-principles simulations, considering both cleavage (100) and polar (110) orientations of SrTiO₃ with distinct terminations, and several adsorption sites for the overlayer. Large charge transfers take place for the two SrTiO(110)/GaAs and O₂-(110)/GaAs polar heterojunctions, at variance with other substrate terminations, which are polar compensated by construction. As a function of the thermodynamic conditions, the formation of mixed compounds at the interface can be avoided. Relying on the interfacial energy, we predict that the GaAs monolayer is much more stable on (110) than on (100) surfaces, consistent with the available experimental results. Moreover, it should wet both SrTiO and Sr terminations of SrTiO₃(110).

DOI: [10.1103/PhysRevB.76.165427](https://doi.org/10.1103/PhysRevB.76.165427)

PACS number(s): 68.35.-p, 68.35.Md, 73.40.Ty, 68.47.Gh

I. INTRODUCTION

Use of polar surfaces as a substrate for growth or growth of ultrathin films that are oriented along a polar direction has become a significant field of research in the past decade. In particular, metal/oxide polar interfaces were extensively studied by experimental means¹ and *ab initio* calculations.²⁻⁵ In these systems, peculiar structural and electronic properties as well as enhancement of adhesion have been pointed out.^{6,7}

As far as semiconductor/oxide interfaces are concerned, the modifications of the electronic structures of the constituents that could be induced by polarity are largely unknown. From the experimental point of view, the preparation of sharp and well ordered interfaces demands the control of the quality of the epitaxy on the polar substrate, as well as of the oxygen interdiffusion, which may result in the formation of mixed compounds with variable stoichiometry. On the other hand, first-principles calculations can take into account the polar nature of the substrate, which has to be compensated,⁸ but must cope with the complexity of several interfacial phases that are possibly stable as a function of the chemical conditions.

Here, we consider the early stage of growth of GaAs on polar SrTiO₃(110) and cleavage SrTiO₃(100) surfaces. SrTiO₃ is attracting much interest for its use in the integration of GaAs optoelectronics with traditional Si-based devices.⁹ SrTiO₃ was employed as a buffer layer, allowing for misfit reduction between Si and GaAs.¹⁰ Although several works focused on Si/GaAs (Refs. 11 and 12) or Si/SrTiO₃ (Refs. 13-16) interfaces, the growth of GaAs on SrTiO₃ substrates has been the object of few experimental studies.¹⁷⁻¹⁹ In particular, the cleavage (100) orientation as well as the polar (110) and (111) surfaces of SrTiO₃ were considered for GaAs growth. The optical quality of the GaAs films has been found to depend on the substrate orientation sensitively; in such respect, SrTiO₃(110) provided the best results.¹⁹ Conversely, SrTiO₃ epitaxial films on GaAs(100) have good crystallinity and the interface is atomically sharp.²⁰ However, no detailed theoretical study of the

GaAs/SrTiO₃ interface has yet been carried out, to our knowledge, and microscopic models for such heterojunctions are lacking. Furthermore, the GaAs/SrTiO₃ system presents specific interest. SrTiO₃(100) is only weakly polar,^{21,22} while GaAs(100) is polar; conversely, the (110) surface of GaAs is nonpolar, while SrTiO₃(110) is polar. Therefore, the structural and electronic properties of epitaxial and well ordered GaAs/SrTiO₃ interfaces are affected by polarity in any case.

Although in the aforementioned experimental works both constituents of the interface are thick enough to be representative of bulk crystals, here we focus on the very early stages of GaAs growth on SrTiO₃ by considering SrTiO₃(100) and (110) (1×1) substrates that are capped by single GaAs monolayers. We show that, even for such a simple system, there are many distinct configurations that are, in principle, stable as a function of the actual chemical environment. We also study the effect of the substrate polarity and the termination of the substrate on the adhesion and structure of the GaAs overlayer. Noteworthy, polarity compensation is needed in macroscopic samples by electrostatics²² and does not necessarily occur in unsupported ultrathin films.²³ Two (100) terminations^{21,24-28} (TiO₂ and SrO) and five (110) polar terminations^{29,30} (SrTiO, O₂, Sr, TiO, and O) are considered. The comparison with bare (1×1) SrTiO₃(110) polar surfaces²⁹ makes it possible to point out the effects on the structural and electronic properties that are due to the adsorption of the GaAs overlayer.

The paper is organized as follows. In Sec. II, we provide the background to simulate a stable ordered GaAs/SrTiO₃ interface: thermodynamic conditions that are needed to avoid the formation of other compounds, epitaxial relationships for GaAs on SrTiO₃, and computational details. In Sec. III, we consider the atomic and electronic structures of a GaAs(100) monolayer, either freestanding or strained at the SrTiO₃ lattice parameter, and its deposition on the TiO₂ and SrO terminations of SrTiO₃(100). In Sec. IV, the deposition of a strained GaAs(110) monolayer on five different terminations of the polar SrTiO₃(110) surface, namely, O₂ and SrTiO, which have the same composition as the bulk layers, and

TABLE I. Experimental formation enthalpy E_i^f in eV/f.u. of various gallium and arsenic oxide compounds i with respect to $\text{Ga}_{(c)}$, $\text{As}_{(c)}$, and $\text{O}_{2(gas)}$ (Ref. 33).

i	GaAs	As_2O_5	Ga_2O	Ga_2O_3
E_i^f	0.736	9.586	3.690	11.288

TiO , Sr , and O , which are polar compensated by construction. In both cases, a systematic investigation of the preferred sites for Ga or As adsorption was carried out, and the electronic structures of the most stable heterojunctions were analyzed, with reference to the separated constituents. The overall stability of the previous configurations as a function of the chemical environment is provided in Sec. V. The adhesion properties of the GaAs overlayer on (100) and (110) oriented SrTiO_3 substrates, with reference to previous experimental works, are finally discussed.

II. THEORETICAL BACKGROUND

A. Conditions for the stability of sharp GaAs/ SrTiO_3 interfaces

In this section, we focus on the thermodynamic conditions that are needed to obtain a sharp ordered interface between GaAs and SrTiO_3 . Indeed, as a function of the growth conditions, oxygen can diffuse and react through the interface, resulting in the formation of a mixed compound and possibly a complex interface with variable stoichiometry. In order to specify such thermodynamical conditions, we follow a previously reported method that has been originally used to determine the stability of the SrTiO_3 compound.³¹

Along the growth process, it is necessary that the SrTiO_3 and GaAs crystals be stable and, at the same time, avoid the formation of binary mixed compounds such as As_xO_y and Ga_xO_y (the ternary compounds $\text{Ga}_x\text{As}_y\text{O}_z$ are not considered here³²). The stability of all those compounds can be compared in terms of the grand potential Ω_i that reads

$$\Omega_i = -E_i^f - N_{\text{As}}\Delta\mu_{\text{As}} - N_{\text{Ga}}\Delta\mu_{\text{Ga}} - N_{\text{O}}\Delta\mu_{\text{O}}, \quad (1)$$

with N_j and $\Delta\mu_j$ the number of atoms and the chemical potential of the j species, respectively. The experimental formation enthalpy E^f of the most common mixed Ga, As, and O compounds is listed in Table I.

By using Eq. (1) and Table I, the stability of the mixed compounds can be easily obtained as a function of the oxygen chemical potential μ_{O} as the independent variable. The regions corresponding to the lowest grand potentials are shown in the left panel of Fig. 1. By merging the stability domains on the lower μ_{O} axis, we obtain that in the O-poor region (1) ($\mu_{\text{O}} < -3.763$ eV), the two elemental As and Ga crystals are stable, while in more O-rich conditions (-3.763 eV $< \mu_{\text{O}} < 0$), the formation of Ga_2O_3 is favored according to thermodynamics. By definition, for $\mu_{\text{O}} > 0$, molecular oxygen is stable, and no stable oxide should be formed. In the right panel of Fig. 1, the computed grand

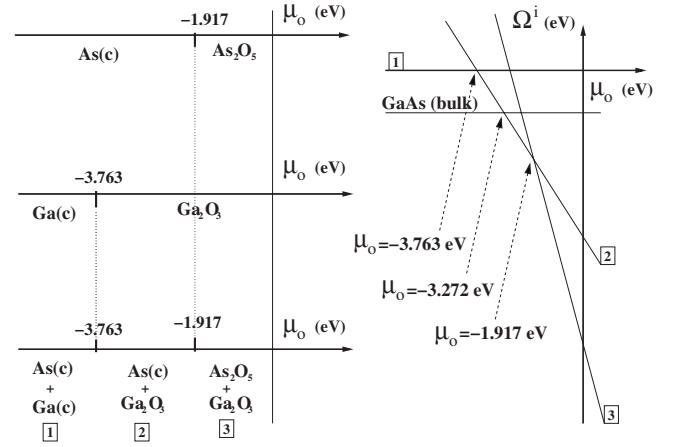


FIG. 1. Left panel: Domains of stability of the GaAs compound with respect to mixed oxides as a function of the oxygen chemical potential μ_{O} . Right panel: Total grand potentials for the three phases (Ref. 1), $\text{As}_{(c)} + \text{Ga}_{(c)}$ (Ref. 2), $\text{As}_{(c)} + \text{Ga}_2\text{O}_3(c)$, and $\text{As}_2\text{O}_5(c) + \text{Ga}_2\text{O}_3(c)$ (Ref. 3) and the bulk one.

potentials of the $\text{GaAs}_{(c)}$, $\text{As}_{(c)} + \text{Ga}_{(c)}$, $\text{As}_{(c)} + \text{Ga}_2\text{O}_3(c)$, and $\text{As}_2\text{O}_5(c) + \text{Ga}_2\text{O}_3(c)$ phases are compared. Bulk GaAs is, thus, stable for $\mu_{\text{O}} < -3.27$ eV.

To summarize, the stability of the GaAs compound in an oxygen external environment (here provided by the SrTiO_3 substrate) is possible if the O chemical potential is lower than -3.27 eV with respect to the O_2 gas phase. The lower bound at $\mu_{\text{O}} < -5.46$ eV is imposed by the stability limit of bulk SrTiO_3 .²⁹ Therefore, a sharp interface between bulk GaAs and SrTiO_3 can be thermodynamically stable with respect to the formation of intermediary oxides if

$$-5.46 \text{ eV} < \mu_{\text{O}} < -3.27 \text{ eV}. \quad (2)$$

Obviously, these considerations apply to bulk phases and take into account neither the influence of kinetics on the interface formation nor the fact that, when depositing GaAs on SrTiO_3 , oxygen is mainly provided by the substrate, so that μ_{O} cannot, in general, be straightforwardly tuned.

B. Epitaxial relationships

The large difference existing between the experimental lattice parameters of GaAs ($a_{\text{GaAs}} = 5.653$ Å) and SrTiO_3 ($a_{\text{SrTiO}_3} = 3.905$ Å) shows that the cube-on-cube epitaxy of these two crystals is not possible. However, if the primitive vectors in the plane parallel to the interface are rotated by 45° (see Fig. 2), the mismatch between GaAs and SrTiO_3 can be reduced to 2.4%.

Along the growing process of GaAs on SrTiO_3 substrates, the stacking sequences of GaAs considered here are:

- (i) along the $[110]$ orientation, thus nonpolar on the polar $\text{SrTiO}_3(110)$ substrate (see Fig. 2, top panel);
- (ii) polar along the $[100]$ on the $\text{SrTiO}_3(100)$ substrate (Fig. 2, bottom panel).

However, many distinct configurations are compatible with such epitaxial relationships. In the case of GaAs/ $\text{SrTiO}_3(100)$, two possible substrate terminations

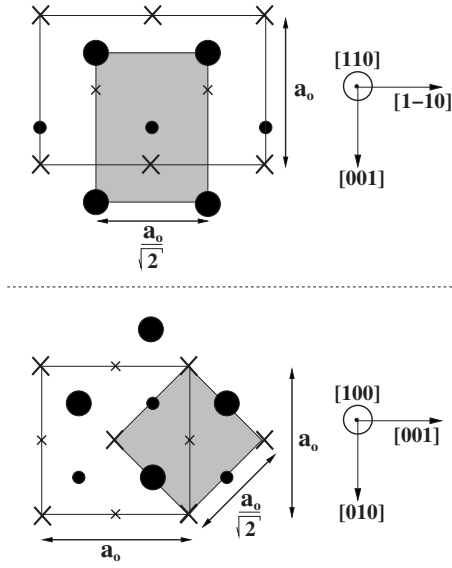


FIG. 2. (1×1) unit cell (shaded area) of the GaAs(110) (top panel) and GaAs(100) (bottom panel) orientations. The gallium and arsenic atoms are represented by black filled circles and crosses. Top panel: Large and small symbols refer to the upper and lower (110) planes, respectively. Bottom panel: Ga (bold circles) and As (large crosses) upper planes; Ga (small bold circles) and As (small crosses) lower planes. The lower and upper (100) planes are mutually shifted by one-half of the surface unit vectors.

(either TiO₂ or SrO) are here considered. Moreover, the GaAs overlayer can be shifted from the center of the substrate surface unit cell along the $[001]_{\text{SrTiO}_3}$ and $[\bar{1}10]_{\text{SrTiO}_3}$ directions (see Fig. 3, right panel), and the contact plane may be formed by either Ga or As. We restrict the number of possible registry shifts by imposing that Ga and As atoms always stand on top of O, Ti, or Sr atoms [no bridge deposition is studied in the case of the (100) terminations].

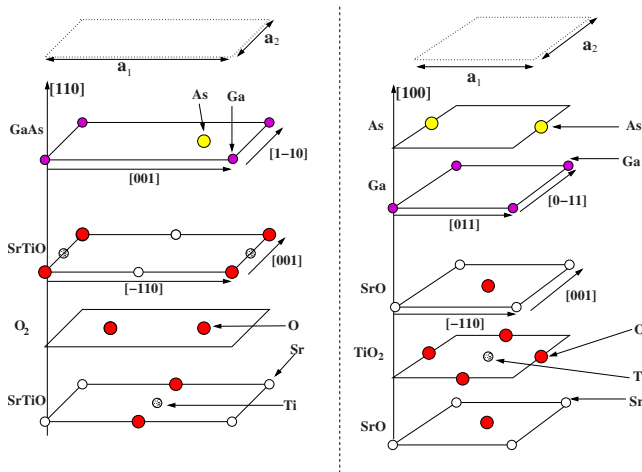


FIG. 3. (Color online) Schematic picture of two starting configurations of a GaAs(110) monolayer on SrTiO₃(110) (left panel) and a GaAs(100) monolayer on SrTiO₃(100) (right panel). In the former case, the GaAs chains are along the $[001]_{\text{SrTiO}_3}$ crystallographic direction.

TABLE II. Theoretical values of the lattice parameter a_0 , bulk modulus B_0 for GaAs and cubic SrTiO₃, and GaAs direct gap. The experimental values are quoted in Refs. 42 and 29. The experimental value of the direct gap is taken from Ref. 43.

	GaAs		SrTiO ₃		
	a_0 (Å)	B_0 (Gpa)	Gap (eV)	a_0 (Å)	B_0 (Gpa)
Theory	5.608	72	0.32	3.951	187
Experiment	5.653	76	1.52	3.903	183

In the case of GaAs/SrTiO₃(110), there are five possible (1×1) substrate terminations, since the outermost SrTiO₃(110) layer may have SrTiO, O₂, Sr, TiO, or O composition.²⁹ As regards the GaAs overlayer, there are four inequivalent positions, which can be obtained by displacing the GaAs chains along the $[001]_{\text{SrTiO}_3}$ or $[\bar{1}10]_{\text{SrTiO}_3}$ directions (see Fig. 3, left panel). In total, 16 and 40 distinct configurations were used as starting points for the geometry optimization of the GaAs/SrTiO₃(100) and GaAs/SrTiO₃(110) interfaces, respectively.

C. Computational details

The calculations are performed in the framework of density functional theory (DFT).^{34,35} Exchange and correlation energy is treated within the local density approximation using the Perdew-Wang parametrization.³⁶ For all calculations, we used the ABINIT computer code.³⁷

Norm-conserving separable pseudopotentials are generated following the Troullier-Martins scheme,³⁸ with reference configurations $3d^{10}4s^24p^1$ for Ga and $4s^24p^3$ for As atoms. The cutoff radii are $R_c(s)=2.09$ a.u., $R_c(p)=2.25$ a.u., and $R_c(d)=2.48$ a.u. for Ga, and $R_c(s)=1.96$ a.u. and $R_c(p)=2.17$ a.u. for As, with s , p , and d the different channels. Therefore, the Ga $3d$ semicore electrons are treated in the self-consistent density (small-core approximation), whereas As $3d$ semicore states are frozen (large-core approximation). The f channel is considered to be local along the pseudization procedure in order to improve the transferability of the pseudopotential and avoid ghost states. Details on Ti, Sr, and O pseudopotentials can be found in Ref. 29. The Kohn-Sham states are expanded in plane wave with 30 hartree cutoff energy. In order to have a symmetric slab and to prevent the formation of a spurious dipole moment,^{39,40} the GaAs monolayer is deposited on two sides of the slab. All the calculations are performed by using a (4,4,4) Monkhorst-Pack mesh⁴¹ for bulk and a (4,4,2) mesh in slab geometry.

The computed lattice parameter a_0 and bulk modulus B_0 of bulk GaAs are within $\pm 1\%$ of the experimental data (see Table II). As regards the epitaxial conditions, the computed misfit between SrTiO₃ and GaAs crystals is equal to $+0.4\%$, which compares quite well to the $+2.4\%$ experimental value. The GaAs lattice parameter a_0 matches the experimental value better than previous calculations [5.56 Å (Ref. 44) and 5.54 Å (Ref. 45)]. The improvement comes from the inclu-

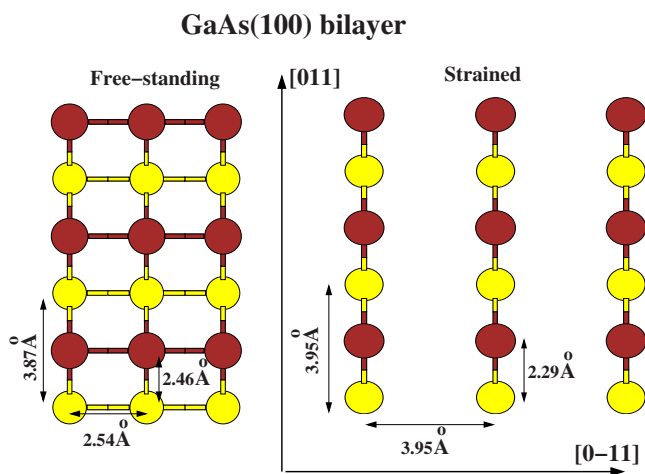


FIG. 4. (Color online) Top view of the freestanding (left) and strained (right) GaAs(100) unsupported monolayers. As and Ga atoms are represented by yellow and brown circles, respectively. The lattice parameters, bond angles, and bond lengths are indicated.

sion of the Ga $3d$ states in the self-consistent charge density calculation. In line with all-electron calculations,^{46,47} the GaAs fundamental band gap is here even more severely underestimated than in previous calculations.^{44,45} Whereas gap underestimation is a well known drawback of DFT,⁴⁸ the use of large-core pseudopotentials with frozen Ga $3d$ electrons increases the fundamental gap with respect to all-electron calculations, thus partly compensating the gap problem. A GW correction to the GaAs DFT fundamental gap using a small-core Ga pseudopotential gives 1.4 eV, close to the experimental value.⁴⁹

III. GaAs MONOLAYER ON SrTiO₃(100)

A. Strained and freestanding GaAs(001) monolayer

As detailed in the previous section, GaAs undergoes a compressive stress upon epitaxy on cubic SrTiO₃, which is slightly underestimated in our calculation. However, such a misfit refers to the interface between two semi-infinite GaAs and SrTiO₃ crystals and does not apply to ultrathin adlayers. Therefore, we also compute the misfit between the GaAs monolayer and the substrate.⁵⁰ As far as the GaAs(100) monolayer is concerned, the misfit is strongly anisotropic and equal to -2.0% and -35.7% along the $[011]$ and $[0\bar{1}1]$ directions, respectively. The strained monolayer is characterized by GaAs chains along the $[011]$ direction with a reduced coordination number (see Fig. 4), while the freestanding monolayer has a rectangular unit cell with both homo- and heteronuclear bonds. Although very large along $[0\bar{1}1]$, such a strain is originated by the peculiar atomic structure of the (1×1) freestanding monolayer with respect to bulklike GaAs(100) planes and is expected to reduce whenever epitaxial growth could proceed.

We have also performed a topological analysis of the electron density⁵¹ as implemented in the ABINIT code. As previously shown, such a method enables us to share the total

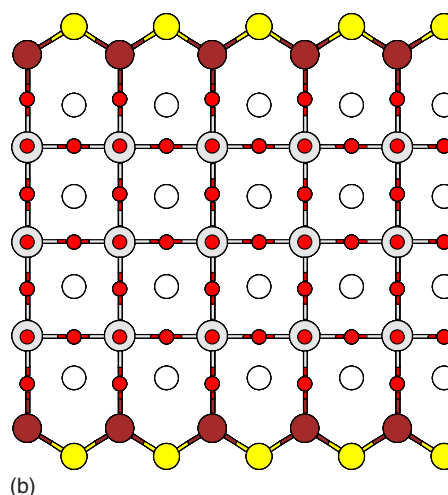
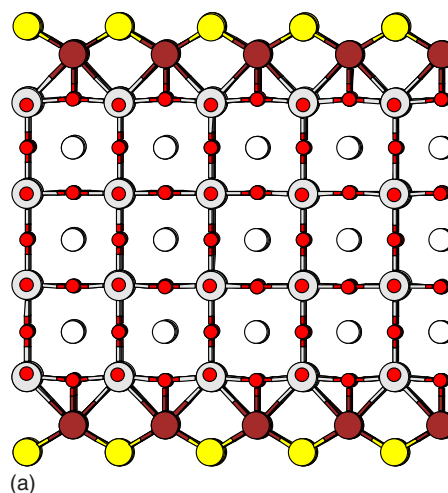


FIG. 5. (Color online) Side view, perpendicular to the $[011]_{\text{SrTiO}_3}$ direction, of the GaAs/TiO₂ (top) and GaAs/SrO (bottom) SrTiO₃(100) interfaces. Ti, Sr, O, As, and Ga atoms are represented by gray, white, red, yellow, and brown circles, respectively.

density among the atomic basins and link them to the modification of the chemical bond.^{29,52} In the freestanding GaAs(100) monolayer, Ga and As topological charges are equal to $\pm 0.37|e|$, thus sensitively reduced with respect to GaAs bulk ($\pm 0.62|e|$). The increased covalent character of the freestanding monolayer is due to the reduced coordination number, which results in a weaker electrostatic potential and a smaller fundamental gap than in the GaAs crystal.

B. (100) GaAs monolayer on a SrTiO₃(100) substrate

After geometry optimization, some of the 16 initial configurations that were described in Sec. II B give the same relaxed structures. In the following, for each termination, we focus on the most stable geometry. In Fig. 5, the two SrO and TiO₂ terminations of SrTiO₃(100) with the lowest interface energy are shown. In both of them, Ga atoms adsorb on top of oxygen, while As atoms stay above the Ga(100) plane and do not bind to the substrate. Indeed, all of the initial configurations that have a contact As plane give rise to less stable

TABLE III. Relaxations of the interplane distance at the GaAs/SrTiO₃(100)-TiO₂ and -SrO interfaces. The mean positions of the layers are computed by averaging the normal coordinates of the atoms belonging to the plane. The interplanar distances are given in Å. For the sake of comparison, the theoretical bulk SrTiO₃ and GaAs interplane distances along the (100) direction are $\frac{a_0}{2} = 1.98$ Å and $\frac{a_0}{4} = 1.40$ Å.

GaAs/TiO ₂ -(100) interface		GaAs/SrO-(100) interface	
Layer	Relaxations	Layer	Relaxations
As		As	
↓	1.17	↓	1.22
Ga		Ga	
↓	2.06	↓	2.03
TiO ₂		SrO	
↓	1.95	↓	1.88
SrO		TiO ₂	
↓	1.98	↓	2.08
TiO ₂		SrO	
↓	1.98	↓	1.98

interfaces. The optimized Ga–O bond length is equal to 1.93 and 1.90 Å in the GaAs/TiO₂- and SrO-(100) cases, respectively, whereas the As–Sr and As–Ti bond lengths are always greater than 3.2 Å. Therefore, the formation of interface Ga–O bond dominates the adsorption process. Such a trend seems to be a characteristic of the GaAs/SrTiO₃ epitaxial interface whenever an equal proportion of Ga and As atoms are deposited.

In Table III, the interplane distances at the interface are listed. As far as the SrTiO₃ substrate is concerned, they are very slightly affected by the GaAs overlayer in the case of the Ga/TiO₂ contact, and show a variation equal to ± 0.1 Å ($\pm 5\%$), with the usual oscillatory damped relaxations, in the case of the Ga/SrO contact. On the other hand, the GaAs interplane distance is similar to the isolated strained monolayer (1.19 Å) and much shorter than in the freestanding monolayer (1.40 Å). Therefore, such a strong interplane distance contraction is not a consequence of the deposition process. Rather, it enables the reduction of the bilayer dipole and the stabilization of the system from electrostatics point of view.²³

The analysis of the topological charges in Table IV shows a moderate electron transfer from the GaAs overlayer to the SrTiO₃(100) substrate, which is equal to $-0.2|e|$ and $-0.11|e|$ for the Ga/TiO₂ and Ga/SrO contacts, respectively. Such a moderate electron transfer is consistent with the weak polar character of the SrTiO₃(100) substrate, which is self-compensated.²¹ On the other hand, the finite dipole of the GaAs overlayer is modified by deposition, which determines the work function variation of the substrate upon GaAs monolayer deposition.

IV. GaAs MONOLAYER ON SrTiO₃(110)

A. Strained and freestanding GaAs(110) monolayer

The atomic structure of the freestanding optimized GaAs(110) monolayer is quite symmetrical, with alternating

TABLE IV. Variation of Bader topological charges (Δq in $|e|$) for the GaAs/TiO₂-(100) and GaAs/SrO-(110) interfaces upon adsorption with respect to bare SrTiO₃(110) and strained monolayer. The layers are indexed starting from the GaAs adlayer (0) going from the surface into the bulk.

Layer	Δq (layer)	Δq (atoms)
GaAs/TiO ₂ -(100) interface		
(0) GaAs	+0.20	Ga: +0.25, As: -0.05
(1) TiO ₂	-0.10	Ti: -0.09, O: -0.01
(2) SrO	-0.02	Sr: +0.01, O: -0.03
(3) TiO ₂	-0.07	Ti: -0.04, O: -0.01
(4) SrO	-0.01	Sr: 0.00, O: -0.01
GaAs/SrO-(100) interface		
(0) GaAs	+0.11	Ga: +0.20, As: -0.09
(1) SrO	-0.07	Sr: -0.04, O: -0.03
(2) TiO ₂	-0.05	Ti: -0.05, O: 0.00
(3) SrO	-0.01	Sr: 0.00, O: -0.01
(4) TiO ₂	-0.03	Ti: -0.03, O: 0.00

Ga–As bonds. As in the case of the (100) GaAs monolayer, the stress corresponding to the epitaxy on SrTiO₃(110) strongly modifies its atomic structure, which shows the characteristic *zigzag* Ga–As chains that appear on the GaAs(110) surface (see Fig. 6). The strong reduction of the lattice parameter leads to a big misfit between the monolayer and the SrTiO₃(110) substrate: -11.1% and -59.1% along the $[001]$ and $[\bar{1}10]$ directions, respectively.

B. GaAs monolayer on a SrTiO₃(110) substrate

1. Atomic structure

The optimized configurations of the GaAs overlayer on the five distinct terminations of the SrTiO₃(110) substrate show contrary features (see Fig. 7). First of all, the GaAs overlayer is atomically flat on the two stoichiometric SrTiO-

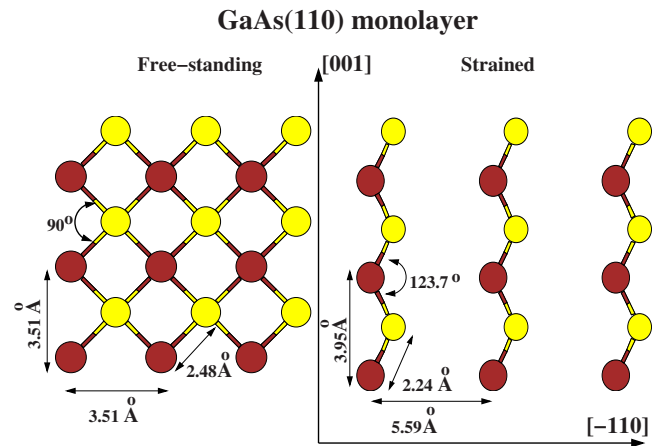


FIG. 6. (Color online) Same caption as Fig. 4, but for the GaAs(110) monolayer.

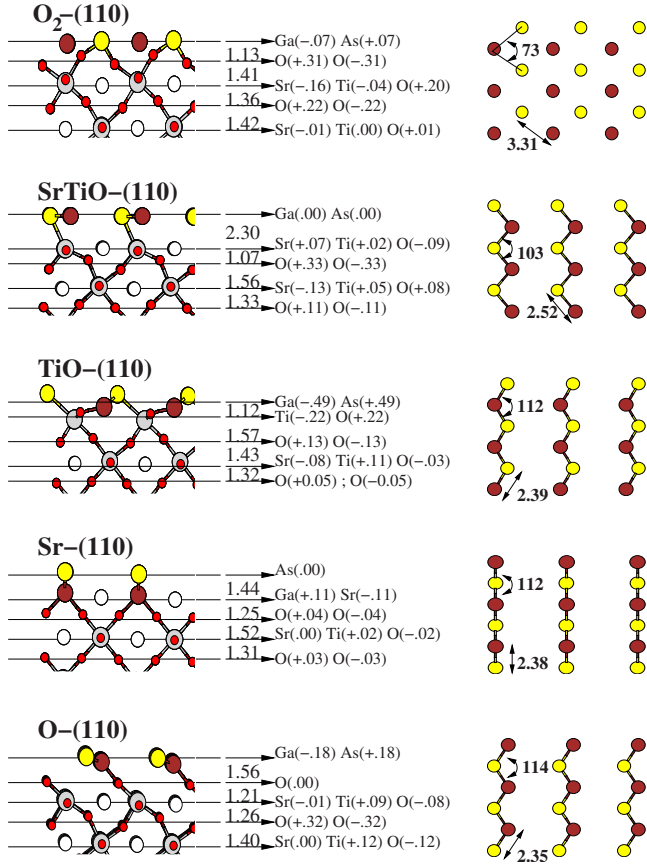


FIG. 7. (Color online) Left panel: Side view, perpendicular to the $[001]_{\text{SrTiO}_3}$ direction, of the GaAs on O₂-, SrTiO-, TiO-, Sr-, and O-SrTiO₃ (110) terminations (from top to bottom), respectively. The interplane distances between the averaged planes are shown between arrows, whereas the atomic rumpling within the layer is listed after the arrow. Right panel: Top view of the GaAs monolayer. Ti, Sr, O, As, and Ga atoms are represented by gray, white, red, yellow, and brown circles, respectively. The GaAsGa angle (in deg) as well as the Ga-As bond lengths (in Å) are also shown.

and O₂-SrTiO₃(110) terminations. At odds, this one is buckled for the two GaAs/O- and GaAs/TiO-(110) interfaces, with rumpling equal to ± 0.18 and ± 0.49 Å, respectively. Vertical Ga-As bonds are obtained on the Sr-(110) termination. Therefore, such a configuration is guessed not to be well suited for the growth of thick GaAs films along the $[110]$ direction.

On the TiO-, O-, and SrTiO-(110) terminations, the Ga-As bond lengths and the GaAsGa angles (see Fig. 7) show similar characteristics. The angles are close to the 109.47° bulk value and the Ga-As chains show bulklike features and are not broken apart upon adsorption, as it is the case on the O₂-(110) termination. For these three interfaces, the Ga-As bond length remains close to the bulk one: $d_{\text{GaAs}}^{\text{Bulk}} = 2.43$ Å. As those three interfaces show Ga-As bond lengths and GaAsGa angles rather close to their bulk counterparts, they are possible candidates for the epitaxial growth of GaAs on SrTiO₃.

Some features of the adsorption geometry cannot be explained by usual arguments based on bond strengths. Indeed,

TABLE V. Same caption as Table IV, but for the GaAs/O₂-(110), GaAs/SrTiO-(110), and GaAs/Sr-(110) interfaces.

Layer	Δq (layer)	Δq (atoms)
GaAs/Sr-(110) interface		
(0) GaAs	-0.04	Ga: +0.38, As: -0.42
(1) Sr	-0.01	Sr: -0.01
(2) O ₂	0.00	O: 0.00
(3) SrTiO	+0.03	Sr: 0.00, Ti: +0.02, O: +0.01
(4) O ₂	0.00	O: 0.00
(5) SrTiO	-0.01	Sr: 0.00, Ti: -0.01, O: 0.00
GaAs/SrTiO-(110) interface		
(0) GaAs	-0.64	Ga: -0.18, As: -0.46
(1) SrTiO	+0.31	Sr: +0.06, Ti: +0.17, O: +0.08
(2) O ₂	+0.25	O: +0.11, O: +0.14
(3) SrTiO	+0.12	Sr: 0.00, Ti: +0.09, O: +0.03
(4) O ₂	+0.05	O: +0.01, O: +0.04
GaAs/O ₂ -(110) interface		
(0) GaAs	+1.54	Ga: +0.21, As: +1.33
(1) O ₂	-1.21	O: -0.60, O: -0.61
(2) SrTiO	-0.12	Sr: 0.00, Ti: -0.05, O: -0.07
(3) O ₂	-0.12	O: -0.05, O: -0.07
(4) SrTiO	-0.14	O: -0.04, Ti: -0.08, Sr: -0.02

the Ga-O bond length is about 1.9 Å for the GaAs/O-, GaAs/TiO-, and GaAs/Sr-(110) interfaces, whereas it amounts to 2.21 and 2.43 Å for the GaAs/O₂- and GaAs/SrTiO-(110) interfaces, respectively. In particular, it is not *a priori* obvious why in the GaAs/O₂-(110) interface As binds to O, while strong Ga-O bonds are formed at the three nonstoichiometric Sr-, O-, and TiO-(110) substrate terminations as in the case of (100) interfaces described in Sec. III A. On the basis of the atomic electronegativity scale, the Ga atom should be more easily oxidized than As, and thus, binds to O. We show in the next section that the changes in the nature of bonding at the interface is a peculiar consequence of the substrate polarity.

2. Electronic structure

In order to explain the trends in the adsorption of a GaAs monolayer on the SrTiO₃(110) substrate, we carry out a comparative charge topological analysis (see Table V) with respect to the clean substrate.²⁹ The behavior of the interface can be rationalized on the basis of the frontier orbitals [that is, the highest occupied molecular orbital (HOMO) and lowest occupied molecular orbital (LUMO) states] of the strained GaAs monolayer and the clean SrTiO₃(110) surface. In the freestanding GaAs monolayer, the computed fundamental gap is almost closed. Both HOMO and LUMO have a pronounced As character. As far as the SrTiO₃(110) substrate is concerned, the cases of the *stoichiometric* and *nonstoichiometric* terminations are analyzed separately. In the former case, polarity compensation takes place by anomalous filling

of surface states, while the nonstoichiometric substrates are self-compensated by construction, and their electronic structure does not depart substantially from bulk SrTiO₃.²⁹ Although quantitatively biased by the poor description of the band offset between GaAs and SrTiO₃ owing to the gap underestimation,⁴⁹ the following description is expected to be qualitatively correct.

On the SrTiO termination, polarity compensation is achieved through filling of a Ti 3*d*-like state at the bottom of the SrTiO₃ conduction band.²⁹ Upon adsorption of the GaAs monolayer, such a state is higher in energy than the As-like LUMO. An electron transfer from the substrate to the adsorbate, thus, takes place, primarily from Ti to As along the interfacial bond, plus a local rearrangement of the topological charges that is due to screening effects. The GaAs layer becomes negatively charged (the layer charge is $-0.64|e|$ as reported in Table V) and the Ga–As bond is slightly dilated, passing from 2.48 to 2.52 Å upon adsorption (see Figs. 6 and 7). The contraction of interfacial As–Ti bonds (2.56 Å) and dilation of Ga–O bonds (2.43 Å) are consistent with the charge modifications.

The O₂ termination of bare SrTiO₃(110) is compensated through the formation of a peroxo O₂²⁻ group, lacking two electrons with respect to the truncation of the bulk plane with formal charges (2O²⁻).²⁹ The corresponding topological surface O charges amount to $q = -0.66|e|$, roughly halved with respect to bulk oxygen ($q = -1.26|e|$). Upon GaAs adsorption, electrons are transferred from the GaAs monolayer to the O₂-(110) terminated substrate, modifying the gallium and arsenic charges: the Ga charge increases by $\Delta q = +0.21|e|$, whereas As charge by $\Delta q = +1.33|e|$. As a consequence of such a charge transfer, the peroxo bond breaks up and As–O bonds (as long as 1.76 Å) with marked ionic character are formed. They are stronger and shorter than Ga–O bonds (2.21 Å). At the same time, the As–Ti bond length increases (3.76 Å) as a result of the electrostatic repulsion between the positively charged As and Ti atoms at the interface.

The nonstoichiometric SrTiO₃(110) Sr, O, or TiO terminations are self-compensated by construction, and no major charge rearrangements happen, as in the case of the SrTiO₃(100) surface. On the three GaAs/TiO-, GaAs/Sr-, and GaAs/O-(110) nonstoichiometric terminations, charge transfers from and/or to the GaAs monolayer are very small (e.g., $\Delta q = -0.04|e|$ for the Sr-GaAs junction in Table V). The overlayer, thus, keeps its almost neutral character and the electronic structure of the substrate is not very much perturbed by the presence of the GaAs overlayer. In this respect, the nonstoichiometric interfaces of GaAs with Sr-, O-, and TiO-terminated SrTiO₃(110) surfaces are similar to the GaAs/SrTiO₃(100) heterojunctions that are described in the previous section.

V. INTERFACIAL THERMODYNAMICS AND ENERGETICS

In this section, the interface energy is examined from various perspectives (see Fig. 8), whether adhesion, adsorption, or wetting properties of the GaAs monolayer on SrTiO₃

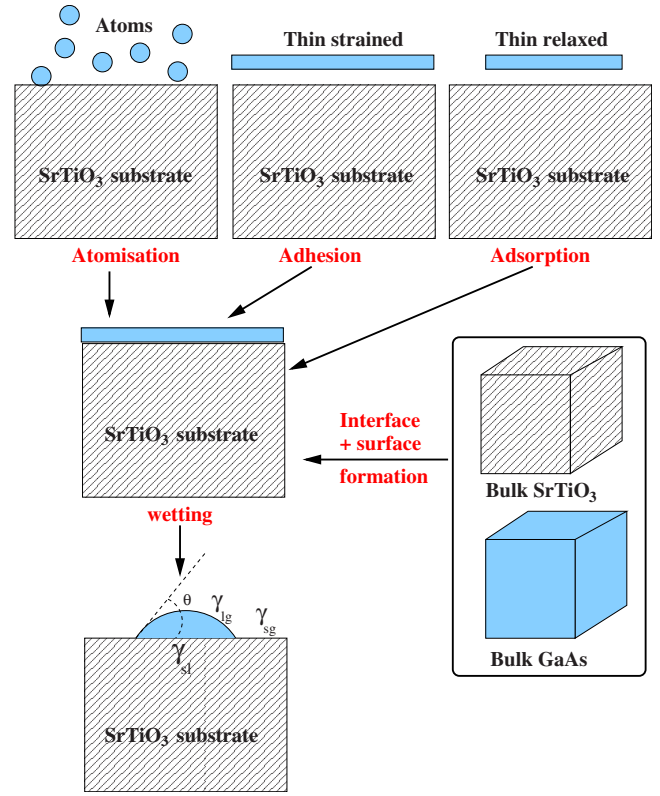


FIG. 8. (Color online) Schematic representation of the atomization, adhesion, adsorption, and interface formation of the GaAs/SrTiO₃ system as well as the wetting of a liquid (l) over a solid (s) in contact with an external environment (g).

substrates are concerned. For each of those properties, we first define the significant quantities to look at, and then discuss the numerical results.

A. Adhesion and adsorption energies

The energy corresponding to the formation of the interface between the GaAs overlayer and the SrTiO₃ substrate can be computed in distinct ways, whether the contributions coming from the stress or interfacial bonds are taken into account. E_{slab}^j and E_{slab}^{ij} define the total energies of the *j*-terminated slab and capped with an *i* monolayer, respectively. Since the following definitions apply to the case of a slab with two symmetric terminations, they include a $\frac{1}{2}$ factor systematically. Formation energies are defined in such a way that they are positive whenever the final state is more stable than the initial one.

The formation energy of the interface by unit area with respect to the isolated atoms *i* (with $i = \text{Ga}$ and As , and E_{atom}^i their total energy) is equal to

$$E_{\text{atom}}^{ij} = -\frac{1}{2A} \left[E_{\text{slab}}^{ij} - E_{\text{slab}}^j - \sum_k^{\text{Ga,As}} E_{\text{atom}}^k \right], \quad (3)$$

with *A* the unit cell area of the (1 × 1) (110) and (100) surfaces. E_{atom}^{ij} (hereafter defined as the *atomization energy*) can be associated with the formation of a GaAs monolayer dur-

TABLE VI. Atomization E_{atom} , adhesion E_{adh} , and adsorption E_{ads} energies of GaAs(110) and (100) monolayers over SrTiO₃(110) and (100) substrates, respectively. $\phi_{\text{int}}^{\text{GaAs/SrTiO}_3}$ are computed by using Eq. (11), whereas $\phi_{\text{surf}}^{\text{SrTiO}_3}$ is taken from Ref. 29. All energies are in J/m² and wetting angles θ in deg.

i/j	E_{atom}^{ij}	E_{adh}^{ij}	E_{ads}^{ij}	ϕ_{int}^{ij}	ϕ_{surf}^j	θ
(110) orientation						
GaAs/O ₂ -(110)	8.63	3.81	3.02	-1.08	1.73	Wetting
GaAs/SrTiO-(110)	6.94	2.12	1.33	3.65	4.78	Wetting
GaAs/O-(110)	6.13	1.31	0.52	0.95	1.27	71.1
GaAs/TiO-(110)	6.45	1.63	0.84	6.24	6.88	49.8
GaAs/Sr-(110)	7.46	2.63	1.84	-4.66	-3.01	Wetting
(100) orientation						
GaAs/TiO ₂ -(100)	8.27	1.43	-0.08	4.84	4.90	87.6
GaAs/SrO-(100)	8.49	1.65	0.14	-2.73	-2.45	78.5

ing molecular beam epitaxy. It takes into account the creation of both interfacial and intralayer bonds in the heterojunction.

The formation energy of the interface by unit area with respect to the i strained GaAs monolayer, with $E_{\text{thin,strained}}^i$ total energy, reads

$$E_{\text{adh}}^{ij} = -\frac{1}{2A} [E_{\text{slab}}^{ij} - E_{\text{slab}}^j - 2E_{\text{thin,strained}}^i]. \quad (4)$$

E_{adh}^{ij} is the *adhesion energy* of the thin film onto the substrate, taking into account the contributions from the creation of interfacial bonds as well as the modifications of the Ga-As bonds when passing from the strained to the supported monolayer.

Finally, we define the formation energy of the interface by unit area with respect to the i freestanding GaAs monolayer with $E_{\text{thin,relaxed}}^i$ total energy as

$$E_{\text{ads}}^{ij} = -\frac{1}{2A} [E_{\text{slab}}^{ij} - E_{\text{slab}}^j - 2E_{\text{thin,relaxed}}^i], \quad (5)$$

which is called *adsorption energy* hereafter. E_{adh} and E_{ads} differ by the elastic energy that is needed to strain the free-standing monolayer to match the substrate lattice parameter. All the results concerning the atomization, adhesion, and adsorption energies are listed in Table VI.

B. Thermodynamics

The thermodynamic stability of GaAs/SrTiO₃(110) and (100) heterojunctions with respect to the bulk crystals is determined by the interface grand potential, which is the interface analog of that previously defined for surfaces.^{29,53} Ω_{int}^{ij} (i =overlayer, j =substrate) is the excess interface grand potential with respect to the SrTiO₃ and GaAs crystals (see the bottom right panel of Fig. 8). Thus, the energies of bulk SrTiO₃ and GaAs (and not the thin film) are used as reference. Accordingly, Ω_{int}^{ij} is computed through the equation

$$\Omega_{\text{surf}}^{\text{thin,GaAs}} + \Omega_{\text{int}}^{ij} = \frac{1}{2} [\Omega_{\text{slab}}^{ij} - N_{\text{SrTiO}_3} \Omega_{\text{SrTiO}_3} - N_{\text{GaAs}} \Omega_{\text{GaAs}}], \quad (6)$$

with N_{SrTiO_3} and N_{GaAs} the number of SrTiO₃ and GaAs bulk unit formulas, respectively. The first term of the left hand

side member, $\Omega_{\text{surf}}^{\text{thin,GaAs}}$, refers to the surface grand potential of the GaAs monolayer, which is in contact with the external environment. It disappears when the system is constructed starting from an interface between two semi-infinite bulk compounds. If the temperature and pressure contributions are neglected, the three bulk grand potentials of the right hand side member are written as

$$\Omega_{\text{slab}}^{ij} = E_{\text{slab}}^{ij} - \sum_k \mu_k N_k,$$

$$\Omega_{\text{SrTiO}_3} = E_{\text{bulk}}^{\text{SrTiO}_3} - \mu_{\text{SrTiO}_3},$$

$$\Omega_{\text{GaAs}} = E_{\text{bulk}}^{\text{GaAs}} - \mu_{\text{GaAs}}, \quad (7)$$

with N the number of atoms, μ the chemical potentials of the various species within the slab, and $E_{\text{bulk}}^{\text{SrTiO}_3}$ and $E_{\text{bulk}}^{\text{GaAs}}$ the SrTiO₃ and GaAs bulk total energies, respectively. In thermodynamic equilibrium, the chemical potentials of strontium titanate μ_{SrTiO_3} and gallium arsenide μ_{GaAs} fulfill

$$\mu_{\text{SrTiO}_3} = \mu_{\text{Sr}} + \mu_{\text{Ti}} + 3\mu_{\text{O}}, \quad (8)$$

$$\mu_{\text{GaAs}} = \mu_{\text{Ga}} + \mu_{\text{As}}. \quad (9)$$

Equation (6) can, thus, be rewritten as a function of the chemical potentials of elemental species and computed energies as

$$\begin{aligned} \Omega_{\text{int}}^{ij} = & \frac{1}{2} [E_{\text{slab}}^{ij} - N_{\text{SrTiO}_3} E_{\text{bulk}}^{\text{SrTiO}_3} - N_{\text{GaAs}} E_{\text{bulk}}^{\text{GaAs}} \\ & - \mu_{\text{Ti}} (N_{\text{Ti}} - N_{\text{SrTiO}_3}) - \mu_{\text{Sr}} (N_{\text{Sr}} - N_{\text{SrTiO}_3}) \\ & - \mu_{\text{O}} (N_{\text{O}} - 3N_{\text{SrTiO}_3}) - \mu_{\text{Ga}} (N_{\text{Ga}} - N_{\text{GaAs}}) \\ & - \mu_{\text{As}} (N_{\text{As}} - N_{\text{GaAs}})] - \Omega_{\text{surf}}^{\text{thin,GaAs}}. \end{aligned} \quad (10)$$

Here, we have knowingly considered a stoichiometric GaAs monolayer ($N_{\text{Ga}} = N_{\text{As}} = N_{\text{GaAs}}$). Consequently, the two last terms in square brackets disappear. Moreover, only two independent variables are needed to define the excess with respect to SrTiO₃ bulk unit formulas [the third one is obtained through Eq. (8)]. As performed in Ref. 29 for the bare sur-

faces, the interface is defined without any titanium excess ($N_{\text{SrTiO}_3} = N_{\text{Ti}}$), which implies the cancellation of the fourth term of the right hand side member. Thus, Eq. (10) becomes

$$\gamma_{\text{int}}^{ij} = \frac{\Omega_{\text{int}}^{ij}}{A} = \phi_{\text{int}}^{ij} - \frac{1}{2A} [\Delta\mu_{\text{O}}(N_{\text{O}} - 3N_{\text{Ti}}) - \Delta\mu_{\text{Sr}}(N_{\text{Sr}} - N_{\text{Ti}})], \quad (11)$$

with

$$\phi_{\text{int}}^{ij} = \frac{1}{2A} \left[E_{\text{slab}}^{ij} - N_{\text{Ti}} E_{\text{bulk}}^{\text{SrTiO}_3} - N_{\text{GaAs}} E_{\text{bulk}}^{\text{GaAs}} - \frac{E_{\text{mol}}^{\text{O}_2}}{2} (N_{\text{O}} - 3N_{\text{Ti}}) - E_{\text{bulk}}^{\text{Sr}} (N_{\text{Sr}} - N_{\text{Ti}}) \right] - \gamma_{\text{surf}}^{\text{thin, GaAs}},$$

where $\Delta\mu_{\text{O}} = \mu_{\text{O}} - \frac{E_{\text{O}_2}^{\text{mol}}}{2}$ and $\Delta\mu_{\text{Sr}} = \mu_{\text{Sr}} - E_{\text{Sr}}^{\text{bulk}}$ are the variation of the chemical potentials with respect to their reference phases (gaseous O₂ and hcp Sr). The computed surface energies $\gamma_{\text{surf}}^{\text{thin, GaAs}}$ of the GaAs(110) and (100) monolayers amount to 0.99 and 1.37 J/m², respectively.

For each substrate termination j , the interface grand potential Ω_{int}^{ij} depends on $\Delta\mu_{\text{O}}$ and $\Delta\mu_{\text{Sr}}$ exactly as the surface grand potential of the clean substrate does. Only the interface-dependent value ϕ_{int}^{ij} differs from its surface counterpart ϕ_{surf}^j , which is given in Ref. 29. For the sake of brevity, we omit in Table VI the dependence on the chemical potentials and provide ϕ_{int}^{ij} versus ϕ_{surf}^j .

C. Wetting

We detail in this section a complementary point of view on the formation of the interface by focusing on the possibility that the GaAs overlayer may wet the SrTiO₃ substrate. The following results are obtained by considering adhesion and wetting between isotropic media. Even if this assumption neglects the anisotropy of the (110) and (100) surfaces, it can be considered as a first step toward more sophisticated approaches.

We begin by a brief reminder before applications to the GaAs/SrTiO₃ interface. The relation defining wetting of an isotropic substrate (s), in contact with an external gaseous (g) environment, by a liquid (l) is the Young equation:

$$\gamma_{\text{sg}} = \gamma_{\text{sl}} + \gamma_{\text{lg}} \cos \theta, \quad (12)$$

with γ_{ij} the surface tension between the i and j phases, and θ the wetting angle in Fig. 8. By using the Dupré relation,

$$E_{\text{adh}}^{l/s} = \gamma_{\text{sg}} + \gamma_{\text{lg}} - \gamma_{\text{sl}}, \quad (13)$$

the celebrated Young-Dupré equation is obtained:

$$E_{\text{adh}}^{l/s} = \gamma_{\text{lg}} (1 + \cos \theta). \quad (14)$$

We proceed along the same way for GaAs/SrTiO₃ interfaces. Equation (13) is rewritten as

$$E_{\text{adh}}^{\text{GaAs/SrTiO}_3} = \gamma_{\text{surf}}^{\text{SrTiO}_3} + \gamma_{\text{surf}}^{\text{thin, GaAs}} - \gamma_{\text{int}}^{\text{GaAs/SrTiO}_3}, \quad (15)$$

which is obviously independent of $\Delta\mu_{\text{O}}$ and $\Delta\mu_{\text{Sr}}$, since the $\gamma_{\text{surf}}^{\text{SrTiO}_3} - \gamma_{\text{int}}^{\text{GaAs/SrTiO}_3}$ difference leads to a cancellation of the chemical potential terms. By using Eq. (11), the adhesion energy [Eq. (4)] can be rewritten as⁵⁴

TABLE VII. Averaged surface energy $\bar{E}_{\text{surf}}^{\text{SrTiO}_3}$ and averaged interface energy $\bar{E}_{\text{int}}^{\text{GaAs/SrTiO}_3}$ in J/m². These quantities are defined in the main text and through Eq. (18).

	$\bar{E}_{\text{adh}}^{\text{GaAs/SrTiO}_3}$	$\bar{E}_{\text{surf}}^{\text{SrTiO}_3}$	$\bar{E}_{\text{int}}^{\text{GaAs/SrTiO}_3}$
O ₂ /SrTiO(110)	2.96	3.25	1.28
O/O(110)	1.31	1.27	0.95
TiO/Sr(110)	2.13	1.93	0.79
TiO ₂ /SrO(100)	1.54	1.22	1.05

$$E_{\text{adh}}^{\text{GaAs/SrTiO}_3} = \phi_{\text{surf}}^{\text{SrTiO}_3} + \phi_{\text{surf}}^{\text{thin, GaAs}} - \phi_{\text{int}}^{\text{GaAs/SrTiO}_3}. \quad (16)$$

At the same time, the wetting angle θ could be computed for each termination and each orientation starting from the Young-Dupré formulation:

$$E_{\text{adh}}^{\text{GaAs/SrTiO}_3} = \gamma_{\text{surf}}^{\text{thin, GaAs}} (1 + \cos \theta). \quad (17)$$

Adhesion energies and wetting angles obtained by using the two previous equations are listed in Table VI.

D. Results and discussion

The values listed in Table VI show a large dispersion as a function of the stoichiometry and/or the orientation of the substrate. However, the trends are not the same whether we focus on atomization, adhesion, or adsorption energy, since each quantity refers to a particular step in the process of deposition. For instance, the atomization energy depends sensitively on the number of Ga-As bonds created per unit area in the overlayer, which is larger for (100) than for (110) orientations.

1. High adhesion energies: Polarity compensation versus replacement of cut bonds

For three interfaces [SrTiO-, O₂- and Sr-(110)], adhesion energy is higher than 2 J/m², whereas the others are around 1.5 J/m². In order to discuss these trends, we average Eq. (16) over complementary terminations of the SrTiO₃ substrate, which are ideally obtained after cleavage: they are O₂/SrTiO, O/O, and TiO/Sr on the polar (110) surface, and TiO₂/SrO ones on (100) orientation. Once averaged, the Young-Dupré equation gives

$$\bar{E}_{\text{adh}}^{\text{GaAs/SrTiO}_3} = \bar{E}_{\text{surf}}^{\text{SrTiO}_3} + \phi_{\text{surf}}^{\text{thin, GaAs}} - \bar{E}_{\text{int}}^{\text{GaAs/SrTiO}_3}. \quad (18)$$

Therefore, the main adhesion energy is enhanced whether (i) the averaged surface energy $\bar{E}_{\text{surf}}^{\text{SrTiO}_3}$ increases or (ii) the averaged interface energy $\bar{E}_{\text{int}}^{\text{GaAs/SrTiO}_3}$ becomes smaller (see Table VII). (i) can be achieved by covering a termination having high surface energy with a smaller energy one, and (ii) can be achieved by lowering the interface energy through the formation of strong interfacial bonds. Obviously, the two processes are not mutually exclusive. An example of mechanism (i) is provided by GaAs deposition on both O₂- and SrTiO-(110) complementary terminations, whose electronic structure is strongly affected by polarity compensation. Mechanism (ii) is instead dominant for GaAs adsorption on

the Sr-(110) termination, owing to the creation of two strong Ga–O bonds (see Fig. 7).

Those two examples show two ways of improving adhesion of ultrathin films on substrates as a function of their polar character and bond formation. The first mechanism is related to the modifications of the electronic structure that are induced by polarity compensation, which in the case of the GaAs/O₂-(110) junction is, here, very effective ($E_{\text{adh}} = 3.81 \text{ J/m}^2$), as also found for various metals on polar surfaces.^{5,6} However, we obtain a larger adhesion energy for the GaAs/Sr-(110) nonstoichiometric junction (2.63 J/m²) than for the GaAs/SrTiO-(110) stoichiometric interface (2.12 J/m²). While the Sr-(110) termination is polar compensated by construction and no major changes of the electronic structure occur, the coordination number of surface Sr is drastically reduced (4 instead of 12 in the bulk). Therefore, the quite large adhesion energy can be mainly attributed in this case to bond formation between highly undercoordinated substrate atoms and adatoms.

2. Adsorption process: (110) polar substrates versus (100) nonpolar ones

For a given orientation, the adsorption energy E_{ads}^{ij} permits defining the stability of an interface with respect to the separated systems—the monolayer (i) and the substrate (j)—including elastic contributions. E_{ads}^{ij} is positive for the five GaAs/SrTiO₃(110) interfaces. Among them, the adsorption energy is rather large for the two stoichiometric GaAs/O₂- and GaAs/SrTiO-(110) heterojunctions, or the nonstoichiometric one GaAs/Sr-(110). Conversely, the adsorption energies are lower for the two GaAs/TiO-(110) and GaAs/O-(110) interfaces and become almost null or negative for the GaAs/SrTiO₃(100) heterojunctions. We conclude that epitaxy of GaAs monolayers on the (100) terminations is not favored.

However, we note that the computed adsorption energies for GaAs/SrTiO₃(110) are generally smaller than for metals on polar oxide surfaces.^{2,5,55–59} Whereas the better screening of the compensating charge in metal than in GaAs overlayers surely influences the adsorption energy, a more thorough understanding of such trends would need a systematic comparison between semiconductor and metal overlayers on polar substrates, which is presently lacking, to our knowledge.

3. Thermodynamic stability of the (110) and (100) interfaces

At variance with E_{ads} , the interface grand potential Ω_{int} provides a measure of the absolute stability of several distinct configurations, possibly differing by stoichiometry, orientation, etc., in the presence of stable bulk phases. Therefore, relying on Ω_{int} , we define the global interface thermodynamic stability rather than the favorable and/or unfavorable process of GaAs adsorption. In Fig. 9, the stability domain diagrams of the five GaAs/SrTiO₃(110) interfaces (top panel) and the two GaAs/SrTiO₃(100) interfaces (bottom panel) are displayed as a function of the O and Sr excess chemical potentials. The domains are obtained by

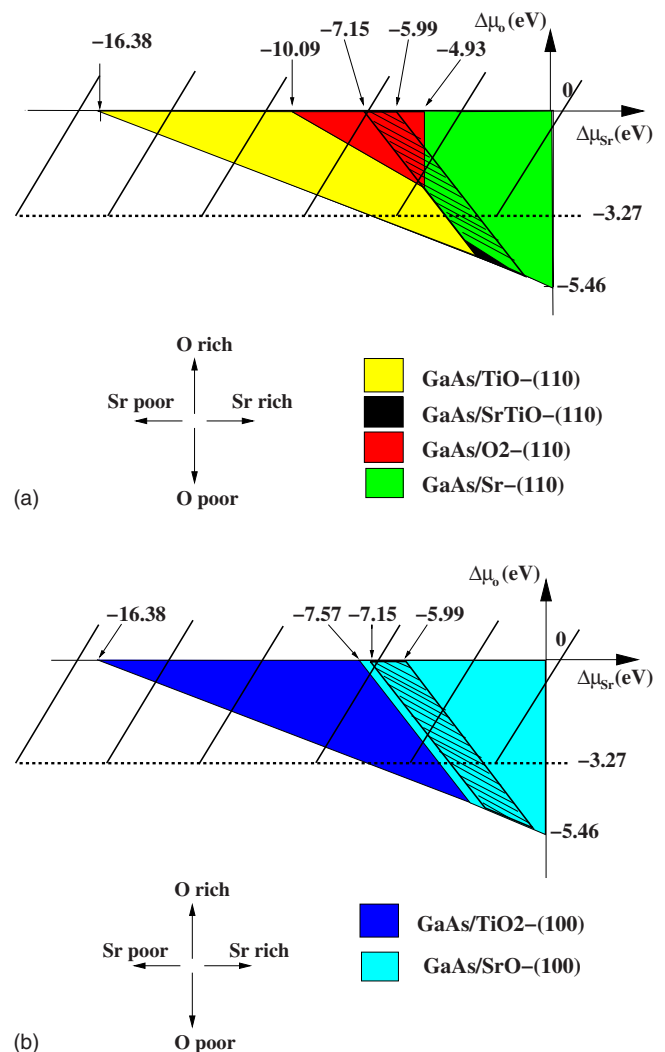


FIG. 9. (Color online) Stability diagram of the five GaAs/SrTiO₃(110) interfaces (top panel) and the two GaAs/SrTiO₃(100) interfaces (bottom panel). The allowed area for mixed Ga_xO_y and As_xO_y compounds is found for $\Delta\mu_{\text{O}} > -3.27 \text{ eV}$. The shaded area corresponds to SrTiO₃ stability with respect to decomposition in SrO and TiO₂.

minimizing, for each $(\Delta\mu_{\text{O}}, \Delta\mu_{\text{Sr}})$ couple, the interface grand potential Ω_{int} . The triangular shape of the diagram is detailed in a previous work.²⁹ An additional shaded area includes the computed domain of stability of bulk SrTiO₃ with respect to precipitation of rutile TiO₂ and rocksalt SrO.^{24,60}

In the top panel of Fig. 9, four interfaces are obtained to be stable. Only the GaAs/O-(110) does not appear. The GaAs/O₂-(110) interface is noteworthy. While the bare O₂-(110) termination is not stable, whatever the external chemical environment,²⁹ it can, in principle, be stabilized by the GaAs overlayer. However, its corresponding domain is obtained in the $(\Delta\mu_{\text{O}}, \Delta\mu_{\text{Sr}})$ region, where the GaAs compound is unstable with respect to the mixed compounds Ga_xO_y and As_xO_y. In order to avoid their formation and to create a sharp interface, a low oxygen chemical potential ($\Delta\mu_{\text{O}} \leq -3.27 \text{ eV}$) must be chosen. As a consequence, only two stable interfaces can be created [GaAs/Sr-(110) and

GaAs/SrTiO-(110)], with GaAs/TiO-(110) marginally stable. Even if the GaAs/O₂-(110) and GaAs/O-(110) interfaces show positive (and even high) adsorption energies, these ones are never stable as a function of $\Delta\mu_{\text{O}}$ and $\Delta\mu_{\text{Sr}}$. Finally, we notice the existence of a small stability domain corresponding to the polar GaAs/SrTiO-(110) interface. For the same reasons as the clean SrTiO-(110) surface, its stability is quite intriguing since the interface electronic structure is strongly modified with respect to bulk SrTiO₃ and GaAs compounds, as shown by means of Bader's topological analysis (see Table V).

In the bottom panel of Fig. 9, we show the thermodynamic stability of the two GaAs/SrTiO₃(100) interfaces. The GaAs/SrO-(110) interface dominates the region without any mixed oxide compounds. If the thermodynamic stability of the GaAs/SrTiO₃(110) and (100) interfaces is directly compared by merging the two panels of Fig. 9, the top one, corresponding to (110)-oriented heterojunctions, is left. Consequently, the GaAs/SrTiO₃(110) interfaces are, in general, more stable than the GaAs/SrTiO₃(100) ones, whatever the thermodynamic conditions. This result highlights the peculiar behavior of the polar SrTiO₃(110) orientation with respect to the cleavage one.

4. Wetting and comparison with experimental results

According to Table VI, the O₂-(110), SrTiO-(110), and Sr-(110) terminations of the SrTiO₃ substrate are totally wet by the GaAs(110) monolayer. Thus, a Franck-van der Merwe two-dimensional (2D) growth is possible on these terminations, whenever the first GaAs layer is not too much distorted from the bulk structure. On the other hand, a Volmer-Weber three-dimensional growth is expected for the GaAs/TiO-(110), GaAs/O-(110), GaAs/TiO₂-(100), and GaAs/SrO-(100) interfaces. Obviously, 2D growth allows thin films with a better crystalline quality to be grown. This conclusion is apparently consistent with the available experimental results. Compared with thin GaAs films grown on SrTiO₃(111) and (100), the optical quality of GaAs film on (110) substrates seems better and even comparable to the GaAs monocrystal.¹⁹ Our theoretical results for the onset of GaAs growth on SrTiO₃ support such experimental findings, as far as well ordered (1×1) unreconstructed substrates are concerned. Among the thermodynamically stable interfaces [mainly GaAs/Sr-(110), GaAs/SrTiO-(110), and GaAs/SrO-(100)], the (110) show high adsorption energies, whereas the (100) is energetically unfavored. On the other hand, two (110) interfaces [GaAs/Sr-(110) and GaAs/SrTiO-(110)] totally wet the substrate, possibly leading to a 2D growth, and are the most stable ones according to thermodynamics.

Regarding the growth of GaAs on SrTiO₃ substrates, our calculations highlight the difficulty of obtaining two-dimensional epitaxial growth of ultrathin ordered and stoichiometric GaAs films. Indeed, SrTiO₃ wetting by GaAs can

be mainly obtained on quite Sr-rich surfaces, which are not among the most stable bare substrate terminations in the same thermodynamic conditions.²⁹ Therefore, we anticipate that a careful handling of the experimental parameters—Sr partial pressure, oxygen flux, and temperature—while depositing GaAs is likely needed for obtaining layer-by-layer epitaxial growth.

VI. CONCLUSION

We have considered in this work the deposition of a GaAs monolayer on a SrTiO₃ substrate by means of systematic density functional calculations. A comprehensive exploration of many distinct configurations of the GaAs/SrTiO₃(110) and (100) interfaces has been carried out, starting from thermodynamically stable SrTiO₃ surfaces. Among them, five GaAs/SrTiO₃(110) interfaces and two GaAs/SrTiO₃(100) interfaces were selected, and their electronic and atomic structures were examined. The interplay of three physical processes on the properties of those interfaces is studied: polarity, stoichiometry, and substrate orientation.

First, we have pointed out the existence of huge charge transfers between the substrate and the adsorbate for the two stoichiometric interfaces GaAs/SrTiO-(110) and GaAs/O₂-(110). This behavior comes from polarity compensation and leads to the localization of the compensating charge at the monolayer. As regards the atomic structure, the Ga atom tends to bind with the substrate and is preferentially adsorbed on the surface oxygen in the case of the nonstoichiometric GaAs/SrTiO₃(110) and GaAs/SrTiO₃(100) interfaces.

Second, we have characterized the interface energetics and shown that the deposition of GaAs on SrTiO₃ is more favored on the polar (110) terminations rather than on the weakly polar (100) ones. Whereas the adsorption energy is almost null and even negative for the (100) substrate, this value sometimes overtakes 1 J/m² and reaches 3 J/m² for [110]-oriented substrates. We also suggest that, contrary to SrTiO₃(100) surfaces, atomically flat GaAs monolayers can be formed, in principle, on Sr- and SrTiO-terminated (110) substrates, for chemical environments that preclude the formation of mixed Ga_xO_y and As_xO_y oxides. However, owing to its atomic structure, the GaAs/SrTiO-(110) heterojunction might be better suited for the epitaxy of thick GaAs films on SrTiO₃. This result is in line with recent experiments emphasizing a better optical quality of GaAs films deposited on SrTiO₃(110) substrates rather than on SrTiO₃(100) ones.

ACKNOWLEDGMENTS

The computer facilities have been provided by the Institut du Développement et des Ressources en Informatique Scientifique (IDRIS/CNRS). The authors thank C. Noguera for very valuable discussions, and acknowledge helpful comments by J.-P. Contour, C. Delerue, J. Goniakowski, P. Sautet, and D. Schmaus.

*francois.bottin@cea.fr

†fabio.finocchi@insp.jussieu.fr

- ¹S. K. Shaikhutdinov, R. Meyer, D. Lahav, M. Bäumer, T. Klüner, and H.-J. Freund, *Phys. Rev. Lett.* **91**, 076102 (2003).
- ²D. J. Siegel, Louis G. Hector, Jr., and J. B. Adams, *Phys. Rev. B* **65**, 085415 (2002).
- ³R. Benedek, M. Minkoff, and L. H. Yang, *Phys. Rev. B* **54**, 7697 (1996).
- ⁴Y. Zhukovskii, E. Kotomin, B. Herschend, K. Hermansson, and P. Jacobs, *Surf. Sci.* **513**, 343 (2002).
- ⁵B. Meyer and D. Marx, *Phys. Rev. B* **69**, 235420 (2004).
- ⁶J. Goniakowski and C. Noguera, *Phys. Rev. B* **66**, 085417 (2002).
- ⁷J. Goniakowski and C. Noguera, *Phys. Rev. B* **60**, 16120 (1999).
- ⁸C. Noguera, *J. Phys.: Condens. Matter* **12**, R367 (2000).
- ⁹B. Lee, J. Oh, H. Tseng, R. Jammi, and H. Huff, *Mater. Today* **9**, 32 (2006).
- ¹⁰R. Droopad, J. Curless, and O. Baklenov, *Inst. Phys. Conf. Ser.* **174**, 1 (2003).
- ¹¹H. M. Tütüncü, G. P. Srivastava, and J. S. Tse, *Phys. Rev. B* **66**, 195305 (2002).
- ¹²J. A. Rodriguez and N. Takeuchi, *Phys. Rev. B* **64**, 205315 (2001).
- ¹³R. A. McKee, F. J. Walker, and M. F. Chisholm, *Phys. Rev. Lett.* **81**, 3014 (1998).
- ¹⁴S. Chambers, Y. Liang, Z. Yu, R. Droopad, J. Ramdani, and K. Eidenbeiser, *Appl. Phys. Lett.* **77**, 1662 (2000).
- ¹⁵R. McKee, F. Walker, M. B. Nardelli, W. Shelton, and G. Stocks, *Science* **300**, 1726 (2003).
- ¹⁶C. J. Först, C. R. Ashman, K. Schwarz, and P. E. Blöchl, *Nature (London)* **427**, 53 (2004).
- ¹⁷Q. Zhao, O. Zsebök, U. Södervall, M. Karlsteen, M. Willander, X. Liu, Y. Chen, W. Lu, and S. C. Shen, *J. Cryst. Growth* **208**, 117 (2000).
- ¹⁸H. Fujioka, J. Ohta, H. Katada, T. Ikeda, Y. Noguchi, and M. Oshima, *J. Cryst. Growth* **229**, 137 (2001).
- ¹⁹C. Ping-ping, M. Zhong-lin, L. Wei, C. Wei-ying, L. Zhi-feng, and S. Xue-chu, *Chin. J. Lumin.* **22**, 161 (2001).
- ²⁰E. A. R. F. Klie, Y. Zhu, and Y. Liang, *Appl. Phys. Lett.* **87**, 143106 (2005).
- ²¹J. Goniakowski and C. Noguera, *Surf. Sci.* **365**, L657 (1996).
- ²²J. Goniakowski, F. Finocchi, and C. Noguera, *Rep. Prog. Phys.* (to be published).
- ²³J. Goniakowski, C. Noguera, and L. Giordano, *Phys. Rev. Lett.* **98**, 205701 (2007).
- ²⁴F. Bottin, F. Finocchi, and C. Noguera, *Surf. Sci.* **550**, 65 (2005).
- ²⁵J. Padilla and D. Vanderbilt, *Surf. Sci.* **418**, 64 (1998).
- ²⁶S. Kimura, J. Yamauchi, M. Tsukada, and S. Watanabe, *Phys. Rev. B* **51**, 11049 (1995).
- ²⁷Z.-Q. Li, J.-L. Zhu, C. Q. Wu, Z. Tang, and Y. Kawazoe, *Phys. Rev. B* **58**, 8075 (1998).
- ²⁸C. Cheng, K. Kunc, and M. H. Lee, *Phys. Rev. B* **62**, 10409 (2000).
- ²⁹F. Bottin, F. Finocchi, and C. Noguera, *Phys. Rev. B* **68**, 035418 (2003).
- ³⁰E. Heifets, R. I. Eglitis, E. A. Kotomin, J. Maier, and G. Borstel, *Phys. Rev. B* **64**, 235417 (2001).
- ³¹A. Pojani, F. Finocchi, and C. Noguera, *Surf. Sci.* **442**, 179 (1999).
- ³²G. Hollinger, R. Skheyta-Kabbani, and M. Gendry, *Phys. Rev. B* **49**, 11159 (1994).
- ³³*CRC Handbook of Chemistry and Physics*, 79th ed., edited by D. R. Lide (CRC, Boca Raton, FL, 1998).
- ³⁴P. Hohenberg and W. Kohn, *Phys. Rev.* **136**, B864 (1964).
- ³⁵W. Kohn and L. J. Sham, *Phys. Rev.* **140**, A1133 (1965).
- ³⁶J. P. Perdew and Y. Wang, *Phys. Rev. B* **45**, 13244 (1992).
- ³⁷X. Gonze *et al.*, *Comput. Mater. Sci.* **25**, 478 (2002).
- ³⁸N. Troullier and J. L. Martins, *Phys. Rev. B* **43**, 1993 (1991).
- ³⁹L. Bengtsson, *Phys. Rev. B* **59**, 12301 (1999).
- ⁴⁰F. Finocchi, F. Bottin, and C. Noguera, *Computational Materials Science* (IOS, Amsterdam, 2003), p. 187.
- ⁴¹H. J. Monkhorst and J. D. Pack, *Phys. Rev. B* **13**, 5188 (1976).
- ⁴²Y.-M. Juan and E. Kaxiras, *Phys. Rev. B* **48**, 14944 (1993).
- ⁴³P. Lautenschlager, M. Garriga, S. Logothetidis, and M. Cardona, *Phys. Rev. B* **35**, 9174 (1987).
- ⁴⁴Jose Luiz A. Alves, J. Hebenstreit, and M. Scheffler, *Phys. Rev. B* **44**, 6188 (1991).
- ⁴⁵M. Sabisch, P. Krüger, and J. Pollmann, *Phys. Rev. B* **51**, 13367 (1995).
- ⁴⁶B. Arnaud and M. Alouani, *Phys. Rev. B* **63**, 085208 (2001).
- ⁴⁷C. Filippi, D. J. Singh, and C. J. Umrigar, *Phys. Rev. B* **50**, 14947 (1994).
- ⁴⁸M. S. Hybertsen and S. G. Louie, *Phys. Rev. B* **34**, 5390 (1986).
- ⁴⁹M. L. Tiago, S. Ismail-Beigi, and S. G. Louie, *Phys. Rev. B* **69**, 125212 (2004).
- ⁵⁰Whenever the atomic structure and the lattice parameters of the monolayer are completely optimized, it will be referred to as the “freestanding monolayer.” Conversely, if the monolayer is strained to match the substrate, while fully relaxing the atomic structure under this constraint, we refer to it as the “strained monolayer.”
- ⁵¹R. Bader, *Chem. Rev. (Washington, D.C.)* **91**, 893 (1991).
- ⁵²C. Noguera, A. Pojani, P. Casek, and F. Finocchi, *Surf. Sci.* **507–510**, 245 (2002).
- ⁵³G.-X. Qian, R. M. Martin, and D. J. Chadi, *Phys. Rev. B* **37**, 1303 (1988).
- ⁵⁴We point out that the adhesion energies obtained according to the Young-Dupré formulation [Eq. (16)] and the more usual approach [Eq. (4)] coincide within numerical accuracy.
- ⁵⁵W. Zhang and J. R. Smith, *Phys. Rev. Lett.* **85**, 3225 (2000).
- ⁵⁶I. G. Batyrev, A. Alavi, and M. W. Finnis, *Phys. Rev. B* **62**, 4698 (2000).
- ⁵⁷A. Asthagiri and D. Sholl, *J. Chem. Phys.* **116**, 9914 (2002).
- ⁵⁸A. Asthagiri, C. Niederberger, A. Francis, L. Porter, P. Salvador, and D. Sholl, *Surf. Sci.* **537**, 134 (2003).
- ⁵⁹A. Asthagiri and D. Sholl, *Surf. Sci.* **581**, 66 (2005).
- ⁶⁰E. Heifets, S. Piskunov, E. A. Kotomin, Y. F. Zhukovskii, and D. E. Ellis, *Phys. Rev. B* **75**, 115417 (2007).